A Wireless Sensor Network for Structural Health Monitoring: Performance and Experience

Jeongyeup Paek, Krishna Chintalapudi, Ramesh Govindan
Computer Science Department
University of Southern California
Los Angeles, CA

John Caffrey, Sami Masri
Civil Engineering Department
University of Southern California
Los Angeles, CA

Abstract

While sensor network research has made significant strides in the past few years, the literature has relatively few examples of papers that have evaluated and validated a complete experimental system. In this paper we discuss our deployment experiences and evaluate the performance of a multi-hop wireless data acquisition system (called Wisden*) for structural health monitoring (SHM) on a large seismic test structure used by civil engineers. Our experiments indicate that, with the latest sensor network hardware, Wisden can reliably deliver time-synchronized tri-axial structural vibration data reliably across multiple hops with low latencies for sampling rates up to 200Hz. This performance was achieved by iteratively refining the system design using a series of test deployments. Our experiences suggested the need for careful* onset detection *in order to preserve the fidelity of the structure's frequency response. Furthermore, the high damping characteristics of large structures motivated an exploration of the processing, sampling, and communication limits of current platforms.*

1. Introduction

Structural Health Monitoring (SHM) focuses on developing technologies and systems that assess integrity of structures such as buildings, bridges, aero-space structures and off-shore oil rigs [1]. Most existing SHM implementations use wired data acquisition systems to collect structural vibration data from various locations in the structure (induced by ambient sources *e.g.,* moving vehicles, winds) for analysis. Installing a large scale wired data acquisition system may sometimes take several weeks and may often turn out to be prohibitively expensive [8]. A *wireless* sensor network based data acquisition system promises enormous benefits such as ease and flexibility of deployment in addition to low maintenance and deployment costs.

There has been an immense amount of research examining various aspects and issues pertaining to sensor network based monitoring networks. However, there have been relatively few reports in the literature on systems implementing a "realistic" application: the work on the Great Duck Island testbed [10, 9] is a noteworthy exception. Such reports not only provide practical validation of sensor network based systems but also chronicle a rich set of experiences and unforeseen system design issues that are useful to the research community in general. In this paper, we validate the performance of Wisden [12] (Section 2), a wireless sensor network data acquisition for structural health monitoring (SHM), by deploying it on a realistic large structure.

Structural monitoring stresses many aspects of sensor network design [12]. It's high data rate requirements exceed the radio bandwidths of the mote-class devices, calling for innovative compression techniques. The application's need for reliable data delivery dictates the need for reliable transport mechanisms that can cope with the packet loss rates commonly reported in wireless deployments. Finally, application requirements motivate the design of lightweight time synchronization schemes. In this paper, we explore two more ways in which the requirements of structural monitoring and the characteristics of real structures influence Wisden's system design (Section 3). We emphasize that these influences were unanticipated, and were discovered only after deploying an early Wisden prototype on a large structure.

The first such discovery was the need to carefully design Wisden's compression technique in order to preserve the fidelity of the structural frequency response. Early versions of the system used a simple run-length encoding technique that attempted to detect and compress periods of inactivity in the structure. We discovered that such a compression technique can "clip" peaks in the structural response, resulting in the removal of higher frequencies from the frequency response. Structural engineers rely on accurate reconstruction of the frequency response. To achieve this, our revised system uses a robust onset-detection technique that

carefully picks out activity periods while preserving the frequency response.

The second discovery was that realistic structures are heavily damped, suggesting the need for higher frequency sampling than we had previously assumed. In theory, since the interesting structural modes are in the tens of Hz, we had assumed it would be sufficient to sample a structure at about 50 Hz. However, in a heavily damped structure, the response to vibrations attenuates quickly (around 0.5 seconds). This results in an insufficient number of samples for robust reconstruction of the frequency spectrum. Thus, a practical version of Wisden needs to sample at higher rates, which stresses the communication and processing limits of mote-class devices.

Finally, we report on the performance of our modified Wisden system on a *seismic test structure*, a full scale model of an actual hospital ceiling complete with plumbing and electrical systems. Seismic activity can be induced in this structure using hydraulic actuators. Our evaluation covers several aspects of Wisden such as data transmission reliability, latency and the gains due to the onset detection scheme. In addition, we also compare the performance of Wisden on two different mote-class platforms, the Mica-2 and the newer Mica-Z. Our evaluations on the seismic test structure show that Wisden can deliver time synchronized vibration data reliably at 200 Hz.

Related Work : We know of two related pieces in the literature that discuss wireless structural data acquisition. Lynch *et al.* [4] designed and fabricated a proof of concept low-power wireless sensing unit and validated it by collecting measurements on the Alamosa Canyon Bridge. The wireless sensing unit can acquire data and transmit it to a base-station over a single hop (*i.e.,* directly to a base station).[1] Such a design constrains sensor node placement significantly. By contrast, Wisden [12] provides autonomous multi-hop reliable data transport, and means for synchronizing sensor data acquired at different sensors.

Mechitov *et al.* [7] have developed a wireless data acquisition system on Mica2 motes for SHM applications. In their implementation authors sample vibrations at 250Hz along a single axis and store it locally. Memory limitations on the mote allows for sampling only for 60 seconds. After sampling the stored data is transmitted reliably over a multi-hop sensor network. The system does not provide time synchronization. Authors have deployed their system on a small scaled model building with 18 floors.

1 several single hop commercial wireless sensing products are also available today *e.g.,www.microstrain.com*.

2. Wisden Overview

In this section, we summarize the design of Wisden for completeness—a more detailed exposition may be found in [12]. Wisden is a system consisting of tens of wireless nodes, placed at various locations on a large structure, to collect and reliably transmit time-synchronized structural vibration data to a base-station. Each Wisden node is a Mica2 or MicaZ mote that measures structural vibrations with the help of a *vibration card* specifically designed for high quality low-power vibration sensing (dynamic range of 1-2 g's, low noise characteristics with 16-bits/sample, 5-20,000 Hz sampling rate with programmable anti-aliasing filter), suitable for SHM applications. Attached to this card is a highly sensitive tri-axial accelerometer (dynamic range of -2.5g-2.5g and a sensitivity in the μg range,) that is capable of sensing up to three channels (3-axes) of vibration data. A *base station* provides the functionality equivalent to a data logger or data acquisition unit, namely the ability to store samples from every sensor.

In Wisden, nodes self-configure to form a tree topology and then send their vibration data to the sink, potentially over multiple hops. The sink usually forwards this data to a base-station (usually a high end PC). Sensors can be seamlessly removed or added in a working Wisden deployment by placing a new node and turning it off/on. Wisden comprises three essential components: *reliable transfer* of vibration samples to the sink; *time-synchronization* of samples generated across various sensor nodes; and *data compression* at the source to relieve bandwidth bottlenecks.

Topology Self-Configuration and Reliable Data Transfer : In Wisden, nodes self-organize themselves into a routing tree rooted at the base station. For this, Wisden leverages the parent selection and tree construction module from the software prototype BLAST [11][2]. Nodes periodically select parents based on packet loss performance (measured both actively using probes and passively using data transmissions) to potential parents.

Wisden implements a NACK-based hybrid hop-by-hop and end-to-end reliability scheme; the former is a necessary performance optimization in wireless networks where link losses up to 30% are not uncommon [13]. For the *hop-by-hop reliability*, nodes infer loss through a gap in the sequence number of sent packets. Nodes overhear transmissions and repair losses from a cache of recently forwarded packets.

End-to-end reliability is required since hop-by-hop reliability scheme cannot recover losses when topology changes or when the packet cache overflows. For the *end-to-end* recovery scheme, a copy of every generated packet is also stored in the source node's EEPROM for re-transmission

2 BLAST is a precursor to the MintRouting TinyOS component.

in case of packet loss. Wisden's base station keeps track of missing packets from all nodes. The base station initiates an end-to-end recovery by using the same mechanism as hop-by-hop recovery, per-hop NACKs.

Data Synchronization : Wisden uses a light-weight approach that focuses on time-stamping the data consistently *at the base station*, rather than synchronizing clocks network-wide as done in protocols such as RBS [2] and TPSN [3]. The Wisden sink synchronizes samples from all the nodes by estimating their generation times according to its own local time. For this Wisden estimates the *residence time* of the received sample (time elapsed between the generation of a sample and its receipt at the sink) and subtracts it from the sample's receipt time at the sink. Ignoring propagation delay of radio waves (on the order of nano-seconds incurred over several hundred meters of path distance to sink) and the clock skew [3] , the residence time of a packet can be calculated by summing the times the packet spent at every intermediate node traversed. Each node calculates the time between receipt of the sample to its eventual successful transmission to the next hop and adds it to a *residence time* field in the packet. The base station (or any node) can thus calculate the time of generation of the samples by subtracting the residence time from its local time.

Data Compression : Finally, to reduce the data-rate and relieve the bandwidth limitations of the motes, Wisden uses a lossy run-length compression scheme at every source. In this scheme, if the difference between the maximum and minimum values of samples over a window is less than a threshold (chosen experimentally to suppress variations due to noise), the variation is considered *insignificant*. For such a window of samples, instead of transmitting all the samples, only their average value is transmitted.

3. Impact of Application Requirements on Design

In this section, we describe how application requirements and the characteristics of realistic structures motivate a re-design of parts of the Wisden system. This re-design was driven by deployment experiences on a seismic test structure (Figure 1). The test structure is a platform for conducting seismic experiments on a full-scale realistic imitation of a 28' $\times$ 48' hospital ceiling. The ceiling is complete with real electric lights, fire sprinklers, drop ceiling installations and water pipes carrying water. Furthermore, the ceiling is designed to support 10,000 lb of weight. The entire ceiling can be subjected to uni-axial motion with a peak-to-peak stroke of 10 inches, using a 55,000 lb MTS hydraulic actuator having a $\pm$5 inch stroke. The hydraulic pump delivers up to 40 GPM at 3000 PSI. The total weight of the moving portion of the test structure is approximately 12,000 lb.

3.1. High Damping Characteristics and Need for High Sampling Rates

The response of any structure can be described as the summation of a set of *modes* (decaying sinusoids at the resonant frequencies of the structure). Typical civil structures have dominant modal frequencies in the range of 0-20Hz. In theory, a sampling rate of 50Hz or higher (Nyquist rate) suffices to capture such frequencies. Considering that lower sampling rates imply lower bandwidth requirements, for our initial set of deployments, we chose a sampling rate of 50Hz.

Our initial deployments revealed an interesting shortcoming of this approach. The hospital ceiling structure is *heavily damped* (see Figure 2) *i.e.*, structural vibrations decay very quickly, within around 0.5 seconds [4]. This is very typical of several real completed civil structures (buildings, bridges *etc.*), since they are specifically designed not to sustain prolonged vibrations. Such a heavily damped system offers a very small time-window in which to collect samples from the response. A sampling frequency of 50 Hz, provides a mere 25-40 samples of useful structural response data - too few for analysis using several SHM techniques (for example performing a Fourier transform on 25-40 samples of data would not provide any useful results for detecting subtle damages in the structure). This leads to the conclusion that *SHM systems deployed on real civil structures demand higher sampling rates than that implied by the Nyquist criterion owing to the heavily damped nature of their structural response*.

3.2. High Frequency Sampling and Limitations of the Platforms

What are the limitations of existing mote-class platforms in supporting high sampling rates? In attempting to quantify these limitations, we encountered a few interesting systems issues. Specifically, we explored the achievable transmission limits of radios on existing platforms, and we examined the impact of EEPROM access latency on the sampling rate. Recall that the EEPROM is used by Wisden to ensure reliable delivery of samples.

3 Crystal skew in Mica motes are experimentally found to be in the order of 10^{-5} at clock frequency of 4.096kHz, which means that timesync error between samples within a packet is on the order of nano-seconds. Since the calculation of the residence time is done on per-packet level, influence of the crystal skew is ignorable in Wisden.

4 The impulse response was generated by inducing a sudden unidirectional shaking movement in the hospital ceiling structure using hydraulic actuators.

Figure 1: Seismic test structure

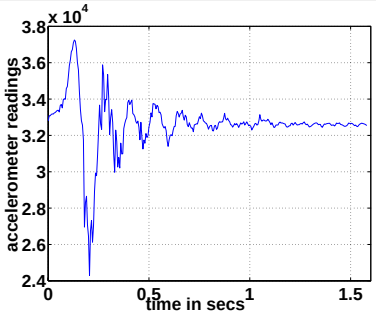

Figure 2: Impulse response of the structure

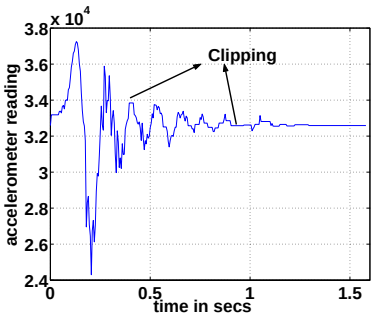

Figure 3: Clippings due to compression in original Wisden.

	Mean (in ms)	**Max** (in ms)	**Std** (in ms)	**Achievable Rate** (r_{max} in pkts/sec)
Mica2	45.09	62.19	5.62	22.17
MicaZ	6.52	12.93	1.75	153.37

Table 1. Packet Transmission Limits

Transmission Rate Limits : The nominal bandwidths for Mica2 (19.2 Kbps) and MicaZ (250Kbps) do not, of course, represent the actual transmission rates achievable by an application. To determine the achievable rates we conducted an experiment with one Wisden node and a sink. For each packet we measured the elapsed time at the application level for a complete packet transmission (in TinyOS terminology, we measured the time from when the application called send() until TinyOS signaled a sendDone()). The distribution of the measured transmission times for Mica2 and MicaZ are shown in Figure 4. Table 1 summarizes the statistics of these times.

In Table 1, the safe achievable rate (calculated using worst case latency) r_{max} is the maximum radio bandwidth a node in Wisden can support. As one might expect, the MicaZ allows approximately an order of magnitude higher packet rate[5]. However, even this platform is woefully inadequate for sustaining the sampling rates required of structural applications. In a worst-case high fanout topology, each node can only safely sustain a sampling rate of 36Hz (single axis) on a 14-node node network. This calculation motivates the need for compression in Wisden; eliminating quiescent periods in structural response can reduce the average data rate requirements to within the capabilities of current platforms. We discuss the design of such compression schemes in Section 3.3.

EEPROM access latency : However, even with a compression scheme that eliminates quiescent periods, mote-class platforms present another bottleneck: the latency of access to the EEPROM. Mica motes use the same bus to communicate with the vibration card and access the EEPROM and these operations have to be mutually exclusive. To access the EEPROM, Wisden must suspend communication with the vibration card and resume it after finishing EEPROM access. During the suspended communication period, incoming samples at the vibration card are buffered until the communication is resumed. Upon resuming the communication, the vibration card transmits all the collected samples to the mote, which then packetizes them and writes them to the EEPROM. The packet generation rate and hence the sampling rate is thus limited by the EEPROM access latencies, which includes the latencies for suspending the vibration card, as depicted in Table II. The worst case latency indicates that we are limited to sampling at no higher than 160Hz, single axis.

While this limit is common to both platforms, the Mica2's radio design, curiously enough, also adversely impacts the achievable sampling rates. The Mica2 transmits one byte at a time over the radio as opposed to MicaZ which operates on a per packet basis. In our implementations we observed that the large rate of interrupts due to high sampling rate interferes with the byte level communication leading to frequent transmission and receiption failures. To alleviate this problem in Mica2, we suspend communication with the vibration card during the packet transmission, further reducing the achievable sampling rate in a Mica2-based Wisden.

This discussion illustrates how seemingly innocuous platform design considerations (EEPROM access latency, radio design) can significantly impact application performance. While compression schemes can alleviate the bandwidth bottleneck and allow for higher sampling rates, sampling rate limits imposed by EEPROM access latencies cannot be avoided. The worst case EEPROM latency indicates that it is safe to operate under a sampling frequency of 160 Hz. In practice, we have found through careful experimentation that while it is possible to sample at 200 Hz without incurring sample losses, rates above 250 Hz result in signif-

5 The size of a Wisden packet is 69 bytes for MicaZ and 66 bytes for Mica2 comprising 59 bytes of payload and header of 10 and 7 bytes for MicaZ and Mica2 respectively.

	EEPROM access time			Packet generation rate limit	Sampling rate limit
	Read/pkt	Write/pkt	Total/pkt		
Average	4.39ms	43.91ms	43.30ms	20.70pkt/s	372.7Hz
Worst case	7.32ms	103.41ms	110.73ms	9.03pkts/s	162.5Hz

Table 2. Sampling rate limit due to EEPROM access

icant losses. As we show in a later section, a sampling rate of 200 Hz seems adequate to reconstruct the frequency response of our heavily-damped seismic test structure.

3.3. Need for Re-designing Wisden's Compression Scheme to Maintain Fidelity of Data

Wisden's original design incorporated a compression scheme that attempted to detect quiescent periods in structural response, while allowing for variations in noise. In this design, a threshold was experimentally chosen to represent maximum variations due to noise, and consecutive samples (two or more) not differing by more than the threshold were compressed into a single value (the average). While the scheme successfully detected quiescent periods, our deployments indicated that it sometimes undesirably modified the structural response during active vibrations.

We discovered two kinds of distortions. First, low-frequency modes are often *clipped* near their maxima/minima. This occurs when the variation of value for low-frequency modes near their maxima/minima may sometimes be small enough to be less than the maximum variation of noise. Second, higher frequency modes in civil structures typically have lower energies and faster decay rates and the original design can eliminate these modes from the response. Figures 2 and Figure 3 depicts these distortions graphically and are obtained from actual measurements on our test structure.

Onset Detection and Data Compression : These distortions motivated a re-design of Wisden's compression technique. In our revised compression scheme we developed an onset detection scheme to detect the start and end of a significant event. Data during this period is transmitted without any compression. At other times, the the original compression scheme is used. This scheme avoids the distortions discussed above, but it's design required significant attention to practical considerations, as we discuss below.

There are several desirable properties of an onset detector: false detections (*i.e.,* occasionally detecting an onset even though there is no significant activity) are permissible but missed detections (missing the starting of a period of significant activity) are not; the onset should be detected as soon as possible after the beginning of the period of significant activity to avoid missing samples; the end of the period should be declared conservatively *i.e.,* only after the structural response has decayed below the noise level; and, the technique should be amenable to memory-and processing-efficient implementation on the motes.

Our onset detector maintains running estimates of three quantities: the noise mean[6] (μ), the noise standard deviation (σ) and, signal envelope (dynamic upper (e^{high}) and lower (e^{low}) bounds of the signal) given by,

$$\mu_i = (1-\beta)s_i + \beta\mu_{i-1}, \quad (1)$$

$$\sigma_i = (1-\beta)|s_i - \mu_i| + \beta\sigma_{i-1}, \quad (2)$$

$$e_i^{high} = max\left(s_i, e_i^{low} + \alpha\left(e_{i-1}^{high} - e_{i-1}^{low}\right)\right), \quad (3)$$

$$e_i^{low} = min\left(s_i, e_i^{high} - \alpha\left(e_{i-1}^{high} - e_{i-1}^{low}\right)\right). \quad (4)$$

Here, s_i, μ_i, σ_i are the values of the sample, mean and standard deviation[7] at the i^{th} time epoch, β is a memory parameter that was chosen using the guideline $\beta^{f_s} = 0.2$ and f_s is the sampling frequency. These choices ensure that the influence of characteristics of data collected one second ago contributes by 20%. For $f_s = 200$ we obtain $\beta \approx 0.99$. The mean and standard deviation are not updated during non-quiescent periods. For choosing α we used the guideline $\alpha^{2f_s} = 0.2$ $f_s = 200$ gives, $\alpha = 0.995$, however due to floating point accuracy restrictions[8] we used $\alpha = 0.99$.

The signal envelope is very sensitive to sudden increases in the signal energy (since it uses *max* and *min* functions) and hence is a good indicator for start of significant activity. The beginning of a non-quiescent period is signaled when $e_i^{high} > \mu_{i-1} + \eta_o\sigma_{i-1}$ or $e_i^{low} < \mu_{i-1} - \eta_o\sigma_{i-1}$ *i.e.,* η standard deviations away from the noise mean. For Gaussian noise, the probability that a noise sample lies beyond η standard deviations from the noise mean is given by $1 - 2erf(\eta)$ *i.e.,* the probability that this sample was not noise is $2erf(\eta)$. Here, $erf(x)$ is the error function of x. Similarly $e_i^{high} < \mu_{i-1} + \eta_q\sigma_{i-1}$ indicates that the maximum value of noise never exceeded a η_q standard deviations from the mean over a history of samples (length of this history is dictated by α. α closer to 1 translates into a longer history), indicating the likelihood that quiescent period has ended.

An important feature of the onset detection scheme is that it does not require memory to store samples and can be used on a sample by sample basis. Figure 5 depicts the functioning of the onset detector on a typical structural response collected from our seismic test structure.

6 Estimating mean continuously is necessary since often sensor readings have an offset, which may depend on environmental conditions.

7 The calculated standard deviation is based on the L_1 norm instead of the L_2 norm since Mica2 and MicaZ motes do not support floating point operations

8 All our fixed floating point operations were limited by 32 bit representations, in this implementation.

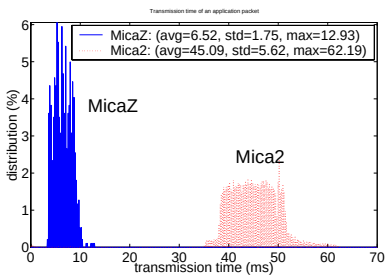

Figure 4: Transmission times distribution for Mica2 and MicaZ

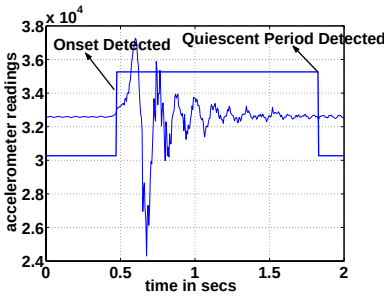

Figure 5: Functioning of the onset detector

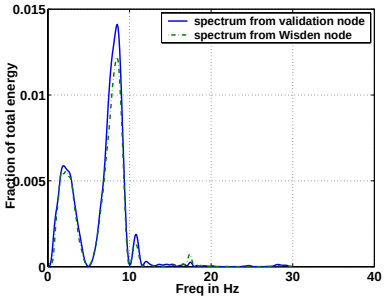

Figure 6: Frequency spectrum of the sensed structural response

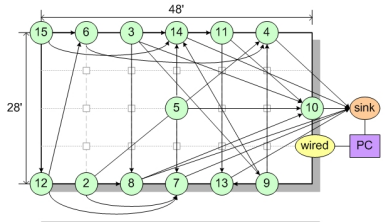

Figure 7: MicaZ 14 node experiment layout

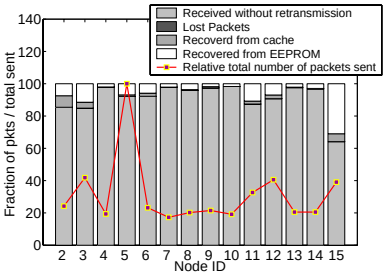

Figure 8: Packet statistics for MicaZ-14node experiment

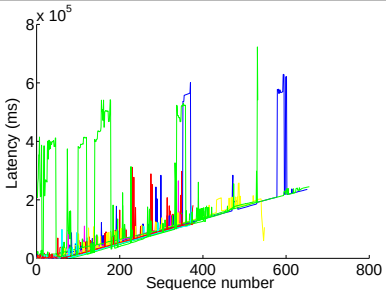

Figure 9: Latency plot of MicaZ-14node experiment

In our initial tests we assumed that the noise characteristics are Gaussian , and chose $\eta_o = 5$ (10^{-5} probability that sample was noise) and $\eta_q = 3$ (0.99 probability that all the samples in the history were noise). However, in our deployments the detector detected too many false positives. Investigation revealed that the noise characteristics differ significantly from Gaussian after the accelerometers are mounted on a Wisden node in that they exhibit periodic spikes and occasionally show large variations. In addition, human motion and vibrations due to motion of heavy objects around the seismic test structure also led to false detections. To compensate for these effects we found the choise $\eta_o = 15$ and $\eta_q = 5$ to work very well. Another effect we observed was that the accelerometer offset takes about 100 seconds to stabilize after being powered on and so it is advisable to warm up the system before starting to collect samples.

These experiences re-inforce the importance of realistic validation of systems designs through experimentation and deployment. Often, unanticipated factors complicate the design of practical systems.

4. System Performance and Characterization

In this section, we evaluate our revised Wisden system by deploying it on the seismic test structure. We start by describing the deployment details and our deployment experiences. We then evaluate the revised system with respect to data integrity and system performance (packet retransmissions, losses *etc.*).

4.1. Our Setup

We evaluated Wisden's performance on a 14 MicaZ node wireless sensor network deployed in the seismic test structure as shown in Figure 7. Nodes 2-15 comprised the wireless sensor nodes in the network and node 1 was the sink. The sink was connected to the base-station (a PC) via a serial port. Accelerometers were secured to the trusses of the structure with double sided tape. A separate validation node (indicated as "wired" in Figure 7) collected vibration samples from the structure (using the same hardware as Wisden) and streamed them directly (without any compression) to the PC over a serial port (without using the radio), and served as a benchmark for our validation.

All Wisden nodes were configured to sample at 200Hz along a single axis parallel to the movement of the structure. Following the discussion in Section 3.2 the packet transmission rate of each node was configured at 2 packets per second. Using the hydraulic actuator, we subjected the structure to two kinds of excitations: impulses and random shaking over a period of about 40 seconds. The system was kept running for about 5 minutes after the forced vibration for the reception of the outstanding vibration data.

4.2. Deployment Experiences

Figure 7 shows the topology of the deployment for the duration of the experiment. Solid lines represent the links that were used by Wisden to route the packets to the sink. If a node has more than one out-going link, that indicates that the topology changed during the experiment and the node changed its parent.

The topology (Figure 7) shows that only 41.3% of the packets were delivered in one-hop, and about half of the nodes formed multi-hop network of 2-4 hops. The average link quality was 91.96%. These findings have two implications. First, even though we have empirically observed radio ranges for the Mica2 and the MicaZ to be up to 100 feet in unobstructed environments, the fact that on the seismic structure whose dimensions were less than 50 feet, the topology selection mechanism picked out multi-hop routes indicates either that the wireless environment was relatively harsh and one-hop links were of poor quality, or that there was significant contention among the nodes (as we shall see later, the latter is the more likely explanation).

Either way, this is an important validation of Wisden's design assumption, and indicates that Wisden will be less sensitive to node placement than systems that assume one-hop wireless delivery of structural data to a base station [5]. Second, it validates the efficacy of the link estimation and topology formation component of Wisden.

An interesting, but perhaps not entirely unexpected, experience was that turning on the hydraulic actuators introduced a significant increase in noise levels and added a static high frequency noise of approximately 100 Hz due to hydraulic dither. We were, however, pleased to note that our onset detector robustly adapted to the noise and dither.

4.3. Data Validation and Onset Detector Performance

In this section we try and validate the data collected from Wisden in both time and frequency domains, using data from the validation node as the benchmark. Note that since these responses are collected from two different locations in the structure and from two different sensors, hence, they will be different. However, their modal content (*i.e.,* modal frequencies of vibration) and onsets should be similar.

Figure 10 and 11 display the sensed vibration data from the validation node and a randomly chosen Wisden node (node 10) respectively. As seen from the figure, all vibration onsets (non-quiescent periods) were accurately detected. Mean square error between the two time series was only 1.13^{-8}g after compensating for the offset in the accelerometers.

Figure 12 zooms into the data and compares one of the impulse responses. Visual inspection indicates the similarity in the modal content of the responses. Figure 12 also demonstrates the success of the onset detector in capturing the response. This figure and Figure 6 shows that the modal content of the two responses is also similar.

4.4. System Evaluation

We now evaluate the overall performance of the Wisden system.

Reliability : As described in Section 2, Wisden uses a combination of hop-by-hop (to reduce latency) and end-to-end delivery schemes. The latter ensures recovery despite topology changes and packet cache overflows. For evaluating Wisden's reliable delivery scheme, during the experiment we measured the fractions of lost packets (ideally, this should be zero), packets that did not require any re-transmissions, packets that were repaired from caches in the hop-to-hop reliability mechanism, and packets there were recovered end-to-end.

These statistics are depicted in Figure 8. The first observation is that Wisden *achieved 100% delivery* (no packets were lost) among a total of 7602 packets. Further we note that all nodes within single-hop from the sink (nodes 4,7,8 and 10) transmitted 95% of the packets without need for any re-transmission. Nodes 15, which was almost always 3 or 4 hops from the sink (also subject to route changes) succeeded in transmitting only 65% of the packets without needing any retransmissions.

9.5% of total packets required retransmission and 2.5% of them were retransmitted more than once. An interesting observation to note is that most re-transmitted packets were recovered end-to-end (7.7%) while only (1.8%) were recovered from cache. We believe the reason for this to be the small size of cache (7 packets) in our current implementation of Wisden due to memory constraints. Increasing the cache size is expected to lower packet delivery latencies for re-transmitted packets, and to result in more frequent hop-by-hop recovery.

Latency : A sampling rate of 200 Hz generates data rate of about 11.1 packets/sec during a non-quiescent period. This is far higher than each node's transmission rate of only 2 packets/sec. The mismatch results in packets being queued up in the EEPROM for transmission and the queue increases at a rate of about 9 packets/sec. The delivery latency of a packet is dictated by the number of packets ahead of it in the EEPROM queue.

This analysis indicates that packet delivery latency will linearly increase with the sequence number of the packet. During a quiescent period the queue is slowly drained and the queue size decreases. This linear increase in latency with increasing sequence number of packets is seen in Figure 9 for every Wisden node. The occasional spikes are a result of increase in latency due to re-transmissions. A con-

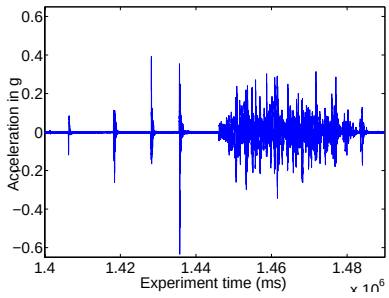

Figure 10: Acceleration data from the validation node

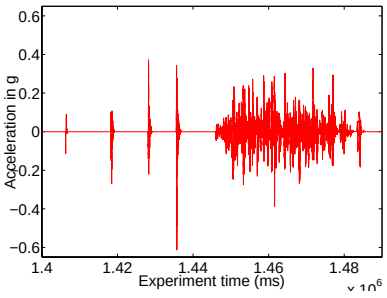

Figure 11: Acceleration data from a Wisden node

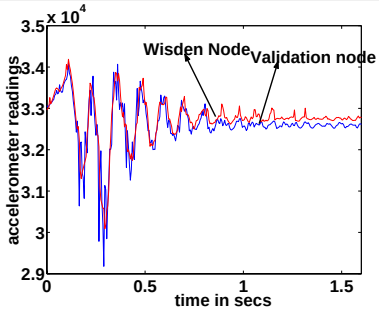

Figure 12: Closeup comparison - validation node vs Wisden node

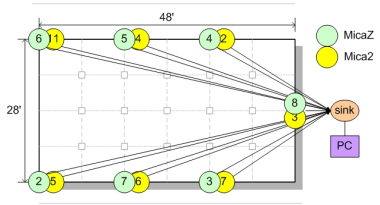

Figure 13: MicaZ-Mica2 comparison experiment layout

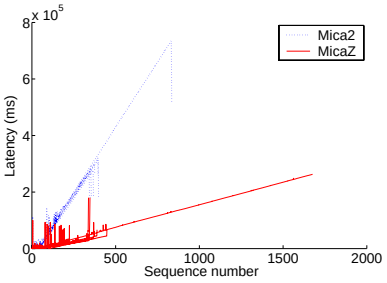

Figure 14: MicaZ-Mica2 Latency comparison plot

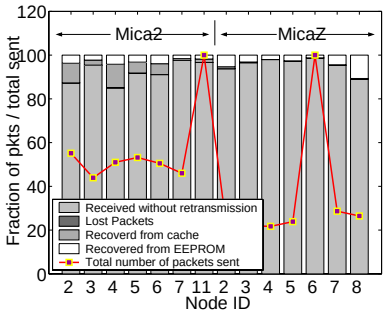

Figure 15: Packet statistics for Mica2-MicaZ comparison

tinuous 1-minute shake results in approximately 667 packets (at 200 Hz) and requires about 6 minutes to completely transmit them.

This indicates a fundamental scaling limitation, since the application requirements outstrip what modern day low-power radios can sustain. As a result, we are investigating hierarchical architectures for the next generation of Wisden design.

Comparison of deployments on Mica2 and MicaZ platforms : Finally, in this section we compare the performance of Wisden deployments on Mica2 and MicaZ platforms. This exercise provides insight into the gains obtained by employing MicaZ motes instead of Mica2 motes. It also reveals some subtle differences between the two platforms.

For this experiment we deployed a 7 node Mica2 and a 7 node MicaZ Wisden network side-by-side as depicted in Figure 13. All the Wisden nodes (for both deployments) were configured to sample at 100 Hz along two axes in the plane of vibration with axis parallel to the direction of movement of the structure. Using the guidelines for choosing node transmission rates discussed in Section 3.2 the packet transmission rates were set at 4 packets per second for MicaZ and 1 packet per second for Mica2. The structure was subject to impulse and random excitations as in Section 4 and both Mica2 and MicaZ deployments collected the vibration data simultaneously.

Figure 13 shows the topology of the deployments during the experiment. Solid lines represent the links that were used by Wisden to route the packets to the sink. We had a single-hop network for 99.7% of the time where all nodes were directly connected to the base station. An interesting observation is that the 14-node MicaZ deployment (see Section 4) had a multi-hop network as opposed to the single hop topology for this experiment even though the dimensions of the structure were same for both deployments. We believe that this was because the contention in the 14-node experiment was higher and the routing mechanism selected a link with better reception rate even if their radio power was high enough to reach the sink directly.

During the experiment, MicaZ nodes had better average link quality (97.8%) than the Mica2 nodes (93.4%). Note that average link quality for Mica2 in the 7 node network was higher than that for the MicaZ nodes in the 14-node experiment (see Section 4). Again, a plausible explanation for this finding is the contention arising from a dense deployment.

Figure 14 compares the observed sample delivery latencies between the two platforms. The slopes of the linear increase in the latency are approximately 5.2 times greater for the Mica2. The average latency during the experiment for the Mica2 was approximately 7 times longer than that of MicaZ [9]

9 This factor of seven can be predicted analytically from the packet generation rate (approx. 11 packets per second), and the configured send-

Figure 15 displays the relative number of packets that were lost, retransmitted using cache, retransmitted using EEPROM, and received without retransmission, for both Mica2 and MicaZ. While the MicaZ deployment required 3.5% of the total packets to be retransmitted, Mica2 required retransmission for 7.2% of the packets. An interesting observation is the difference in the behavior of how the two platforms recovered the lost packets. Figure 15 indicates that the MicaZ deployment mainly relied on the recovery from the EEPROM (3.3% as opposed to only 0.2% from the cache) whereas the Mica2 deployment was able to make use of the caches more efficiently (4.4% as opposed to 2.8% recovery from the EEPROM). We believe the reason for this is the much higher transmission rate of the MicaZ deployment as compared to that of the Mica2 deployment, while their cache sizes being the same. Since MicaZ was sending faster, the caches were being over-written more frequently.

5. Conclusions

This paper describes the rich set of experiences gained while deploying Wisden- a complete data acquisition system for SHM applications, in a real environment. Iteratively refining the system design through series of test deployments helped us in designing a novel onset detection scheme which allowed Wisden to overcome the bandwidth constraint and achieve higher frequency sampling. Our evaluations on the seismic test structure show that Wisden can deliver time synchronized vibration data reliably at a sampling frequency of 200 Hz. The collected data helped us in determining the dominant modal frequencies of the structure. Our comparison of Wisden deployments for the Mica2 and MicaZ platforms, and our exploration of the sampling and data rate limits of these platforms indicate that low-level design decisions often have surprising effects on application performance.

References

[1] S. W. Doebling, C. R. Farrar, M. B. Prime, and D. W. Shevitz. Damage Identification and Health Monitoring of Structural and Mechanical Systems from Changes in their Vibration Characteristics: A Literature Review. Technical report, Los Alamos National Laboratory, May 1996.

[2] J. Elson, L. Girod, and D. Estrin. Fine-grained network time synchronization using reference broadcasts. In *Proceedings of the Fifth Symposium on Operating Systems Design and Implementation (OSDI 2002)*, Boston, MA, 2002.

[3] S. Ganeriwal, R. Kumar, and M. B. Srivastava. Timing-sync protocol for sensor networks. In *Proceedings of the first international conference on Embedded networked sensor systems*, pages 138–149. ACM Press, 2003.

[4] J. P. Lynch, K. H. Law, A. S. Kiremidjian, T. W. Kenny, E. Carryer, and A. Partridge. The Design of a Wireless Sensing Unit for Structural Health Monitoring. In *Proc. of the 3rd International Workshop on Structural Health Monitoring*, Stanford, CA, USA, September 2001.

[5] J. P. Lynch, A. Sundararanjan, K. H. Law, A. S. Kiremidjian, E. Carryer, H. Sohn, and C. H. Farrar. Field Validation of a Wireless Structural Monitoring System on the Alamosa Canyon Bridge. In *SPIE's 10th Anuual International Symposium on Smart Structures and Materials*, San Diego, CA, USA, March 2003.

[6] A. Mainwaring, J. Polastre, R. Szewcyk, D. Culler, and J. Anderson. Wireless Sensor Networks for Habitat Monitoring. In *Proceedings of the Workshop on Wireless Sensor Networks and Applications*, Atlanta, GA, USA, September 2002.

[7] K. Mechitov, W. Kim, G. Agha, and T. Nagayama. High-Frequency Distributed Sensing for Structure Monitoring. In *Proc. of the First International Conference on Networked Sensing Systems*, Tokyo, Japan, June 2004.

[8] E. G. Straser and A. S. Kiremidjian. A Modular, Wireless Damage Monitoring System. Technical report, John A. Blume Earthquake Engineering Center, Department of Civil and Environmental Engineering, Stanford University, Stanford, CA, USA, 1998.

[9] R. Szewczyk, A. Mainwaring, J. Polastre, J. Anderson, and D. Culler. An analysis of a large scale habitat monitoring application. In *Proceedings of the Second ACM Conference on Embedded Networked Sensor System*, November 2004.

[10] R. Szewczyk, J. Polastre, A. Mainwaring, and D. Culler. Lessons from a sensor network expedition. In *Proceedings of the First European Workshop on Wireless Sensor Networks*, January 2004.

[11] A. Woo, T. Tong, and D. Culler. Taming the Underlying Challenges of Reliable Multihop Routing in Sensor Networks. In *Proceedings of the First ACM Conference on Embedded Networked Sensor Systems (SenSys 2003).*, Los Angeles, CA, November 2003.

[12] N. Xu, S. Rangwala, K. Chintalapudi, D. Ganesan, A. Broad, R. Govindan, and D. Estrin. A Wireless Sensor Network for Structural Monitoring. In *Proceedings of the ACM Conference on Embedded Networked Sensor Systems*, Baltimore, MD, USA, November 2004.

[13] J. Zhao and R. Govindan. Understanding Packet Delivery Performance In Dense Wireless Sensor Networks. In *Proceedings of the ACM Conference on Embedded Networked Sensor Systems*, Los Angeles, CA, USA, November 2003.

ing rate differences between the two platforms. We have omitted this analysis for brevity.